FABRICATION OF HIGHLY FLEXIBLE STRAIN SENSOR BASED ON ELASTOMER/MXene COMPOSITES

HARUNA ABBA USMAN, BSc.

Submitted in fulfillment of the requirements
for the degree of Master of Science
in Mechanical & Aerospace Engineering

NAZARBAYEV UNIVERSITY

School of Engineering and Digital Sciences
Department of Mechanical & Aerospace Engineering
Nazarbayev University

53 Kabanbay Batyr Avenue,
Nur-Sultan city, Kazakhstan, 010000
Supervisor: Assistant Professor Sherif Araby Gouda
Co-supervisor: Assistant Professor Gulnur Kalimuldina

April 2023

DECLARATION

I affirm that the manuscript titled "*Fabrication of highly flexible strain sensor based on elastomer MXene*" is the outcome of my original work, with the exception of appropriately acknowledged quotations and citations. Furthermore, I confirm that, to the best of my knowledge and belief, this manuscript has not been previously or concurrently submitted, either in its entirety or in part, for any other degree or diploma at Nazarbayev University or any other national or international institution.

Haruna

Name: Haruna Abba Usman

Date: 07.04.2023

ABSTRACT

Flexible strain sensor has gained popularity in recent years due to high demand in modern applications such as flexible electronics, IoT, human-machine interactions, human-motion detection and structural health monitoring. Usually, metal layers made of silver, copper and other metals were deposited to create strain sensors. Nevertheless, they are frequently made from non-stretchable substrates, they have a restricted ability to be elongated for large strains; therefore, they are not durable at large strain range and are susceptible to mechanical faults. In the present work, we investigate the fabrication of a highly flexible strain sensor based on ternary composites; PDMS/MXene/CNTs composite. MXene (2D material) and multi-walled carbon nanotubes (MWCNTs, 1D material) are added *via* solution mixing as conductive nanofillers into a flexible matrix; poly(dimethylsiloxane). X-ray diffraction, Raman spectra and scanning electron microscopy are employed to study chemical morphology and microstructure of the developed film. Gauge factor – sensitivity to mechanical strain− is recorded as high as 7. The developed sensor was durable and reliable with no significant deterioration over 10^3 cycle. Sensing various human movements is also investigated showing high sensitivity to elbow bending, and knee and wrist movements. The study shows that integrating 2D and 1D materials as two-phase conductive nanofillers is a promising strategy to develop highly strain-sensitive and yet flexible nanocomposites.

Keywords: Strain sensor; MXene; Multi-walled carbon nanotubes; Conductive composites

ACKNOWLEDGEMENT

Alhamdulillah, I would like to begin by conveying my heartfelt thanks and gratefulness to my supervisor, Assistant Professor Sherif Araby Gouda, and my co-supervisor, Assistant Professor Gulnur Kalimuldina, for their unwavering and consistent support and motivation throughout my academic journey and research. Their guidance, expertise, and understanding have been invaluable to me during the entire research process. I am truly appreciative of all that they have done for me and cannot imagine having better mentors for my research.

I express my sincere appreciation to Professor Essam Shehab, who serves as the head of our department, and Assistant Professor Md Hazrat Ali for their encouraging words and insightful guidance throughout my period of study. Furthermore, I want to acknowledge and thank my colleagues and senior researchers at the Department of Mechanical and Aerospace Engineering and Assistant Professor Gulnur Kalimuldina's research team for their continuous support and direction.

Finally, I want to genuinely convey my appreciation to my family members and friend who have provided me with support and motivation throughout my entire academic journey.

Table of Contents

ABSTRACT 2
ACKNOWLEDGEMENT 3
List of Figures 5
List of Tables 5
CHAPTER 1 6
INTRODUCTION 6
1.1 Introduction 6
1.2. Motivation and Problem Statement 7
1.3 Research Aims and Objectives 7
CHAPTER 2 8
LITERATURE REVIEW 8
2.1 Introduction 8
2.2 MXene: New 2D Material 9
2.3 Strain Sensors based on MXene/Polymer nanocomposites 10
CHAPTER 3 15
EXPERIMENTS AND METHODOLOGY 15
3.1. Materials 15
3.2. Synthesis of MXene 15
3.3. Modification of MWCNTs and preparation of $Ti_3C_2T_x$-MXene/m-MWCNTs 16
3.4. Fabrications of m-MWCNT/MXene/Ecoflex composite strain sensor. 17
CHAPTER 4 19
RESULTS AND DISCUSSION 19
4.1 Chemical morphology and microstructure 19
4.2. Mechanical measurements 21
4.3. Electromechanical performance of MXene-based composites 22
4.4. Real-Time Application human movement 27
CHAPTER 5 29
Conclusions 29
Reference 30

List of Figures

Figure 1. MAX phase and MXene production elements are shown in the periodic chart[26]..... 10
Figure 2. (a) preparation of polyurethane/MXene strain sensor, (b) digital image of polyurethane/MXene strain sensor, (c,d) SEM micrographs of polyurethane/MXene with interconnecting structure, and shriveled structure respectively [47]..... 11
Figure 3. (a) Schematic illustrating synthesis of MXene incorporated with CNT layer; (b) Tyndall effect of MXene and SWNT suspension, (c,d) TEM images micrograph of MXene And SWNT, respectively, (e) strain sensor at different percentages [54]. 13
Figure 4. (a) relative resistance-strain curve; (b) resistance variation, (c) resistance response, (d) resistance response at various frequencies, (e) resistance with strain as a function of time, (f) durability test [54]. .. 14
Figure 5. Schematic representation of MXene synthesis. 16
Figure 6. Representation of modification of MWCNTs 16
Figure 7.Schematic representation of preparation of MXene/m-MWCNTs composite 17
Figure 8. Fabrication of strain sensor sample using m-MWCNT/Ecoflex 18
Figure 9. (a) XRD pattern of MXene, MWCNT and MXene/MWCNT, (b) FTIR Spectra of MXene, MWCNT and MXene/MWCNT. 20
Figure 10. SEM images; (a) MAX phase powder; (b) MXene nanosheet, (c) MWCNT, (d) m-MWCNT, (f) MXene/MWCNT 20
Figure 11. Mechanical measurement setup 21
Figure 12. Mechanical properties of MXene/m-MWCNT/Ecoflex: Tensile strength. 22
Figure 13. Electromechanical station to test strain sensitivity of Ecoflex/MXene/MWCNTs composite .. 23
Figure 14. Relative resistance-strain curve within 0-60% at of $Ti_3C_2T_x$MXene, and $Ti_3C_2T_x$MXene/m-MWCNTs..... 25
Figure 15. (a) MXene /m-MWCNTs strain sensor stretched at 10% strain with different frequencies (0.01Hz, 0.05Hz, 0.1Hz, 0.2Hz and 1Hz); (b) MXene /m-MWCNTs strain sensor stretched at 30% strain with different displacement rate (0.0025 m/s, 0.005 m/s, and 7 m/s), (c) MXene /m-MWCNTs strain sensor stretched at 15%, 30% and 45% strain. 26
Figure 16. Cyclic tensile test for MXene/m-MWCNTs strain sensor at 10 % strain 27
Figure 17. Detecting human body motion using MXene /m-MWCNTs strain sensor: (a) Digital photograph of finger bending; (b) finger bending graph, (c) Digital photograph of hand wrist motion, (d) Hand wrist motion graph, (e) Digital photograph of Knee bending movement, (f) Knee bending graph. ..... **Error! Bookmark not defined.**

List of Tables

Table 1.comparison of strain sensor made from different materials 25

CHAPTER 1

INTRODUCTION

1.1 Introduction

A sensor is a device that transforms a physical input into an output that is functionally linked and typically takes the form of signal (either electrically or optically) that is able to read or recognized whether by individual operators as well as electric device [1]. Force, pressure, temperature are examples of entities that can be measure by sensors and their related interface [2]. A sensor is primarily defined as a device that is only responsive to the physical or chemical quantity to be measured and does not affect the characteristics of the physical or chemical quantities while it is operating [3]. These sensors are unresponsive to all other variables that are likely to occur in their application. The responsiveness of a sensor describes how much the output can vary depending on how the chemical and/or physical characteristic being measured changes. Specificity, responsiveness, precision, calibration range, sharpness, cost-effectiveness, durability, and other crucial characteristics of a sensor should all be taken into account while choosing one, in addition to the current environmental factors [4].

Sensors can be broadly divided into two categories based on the characteristics of the material or sample being measured: physical and chemical. The physical category includes devices that detect or measure physical responses such as force, pressure, temperature, index of refraction, magnetic and electrical properties [5]. In addition, there is no chemical interface with the instruments. A chemical sensor possesses chemically sensitive surface that reacts only to a specific sample [6].It focuses specifically on the chemical data gleaned from the analyte's chemical response or a physical characteristic of the system under investigation. The concentrations of a particular element or the investigation of the entire composition may be included in this data, which is subsequently converted into signals with analytical applications such as conductance, light, voltage, current.

Depending on the perspective of signal conditioning, sensors can also be categorized as either passively or actively [7]. An active sensor is one that needs an external source of stimulation, such as laser fluorosensor, synthetic aperture radar, sonar and resistive strain gauge pressure sensors. These sensors do not produce output without the external source. In contrast to active sensors, a

passive sensor produces their own energy or obtain from their related components being used, negating the need for an external power source. Piezoelectric, thermocouples are examples of passive sensor.

1.2. Motivation and Problem Statement

Generally, a flexible strain sensor is made of up conductive materials incorporated in soft stretchable materials (elastomers). A strain sensor should meet certain requirement such as high gauge factor, responsiveness, longevity, linearity, and low hysteresis in order to function in an ideal manner. Many research experiments have been conducted using different conductive material in order to manufacture flexible strain sensor but still its huge challenge to have ideal sensor with aforementioned qualities. In order to achieved such qualities we are investigating the fabrication of flexible strain sensor by integrating the conductive materials with various morphologies (1D and 2D materials) to have joint composite conductive film.

1.3 Research Aims and Objectives

The main aim of the work is to fabricate highly flexible strain sensor based on elastomer (Ecoflex) as substrate. MXene (2D material) with MWCNTs (1D material) conductive materials are used to form a 3D conductive network within the elastomeric matrix. The objectives of this research work are as follows:

- To synthesize MXene nanosheet from MAX phase powder using chemical etching approach.
- To chemically modify MWCNTs to promote its dispersion with the elastomeric matrix
- To synthesis elastomer/ MXene composites and elastomer/MXene/MWCNT composites
- To investigate microstructure and morphology of the developed composites
- To study strain sensitivity of the developed composites and their durability

CHAPTER 2

LITERATURE REVIEW

2.1 Introduction

Recently, there are surged in demand of flexible and wearable electronics such as flexible batteries [8], stretchable circuits [9], soft robot [10], electronic skin [11], supercapacitor [12], and flexible sensors [13]. Specifically flexible and stretchable strain sensor has attracted extensive attention from the researchers working in different areas such as smart healthcare monitoring [14], human-machine interface and entertainment control [15]. Due to high and efficiency mechanical deformation-electrical signal conversion, flexible and stretchable strain sensor can easily be employed to detect human motion, real-time health care monitoring and human-machine interaction. Flexible and stretchable strain sensors are fabricated from soft and flexible sensing and substrate materials composed with stretchable elastomers [16]. An ideal strain sensor must meet some relevant requirements such as high efficiency, high sensitivity, large stretchability (Gauge factor), fast response and recovery, reliable durability, linearity and low hysteresis [17]. From the requirement mentioned, high sensitivity is the most important factor in various applications such as human motion detection. Additionally, robust and conformal environmental stability of the strain sensor should be enough to withstand daily human activities. Exponential progress have been made for fabrication of strain sensor. Various conductive materials have been studied in order to fabricate high sensitivity and stretchability strain sensor such materials are carbon nanotubes [18], carbon black [19], metal nanowires [20], metal nanoparticles [21], and graphene [22]. However, it's challenge to develop an appropriate process of fabricating strain sensor with high sensitivity, excellent stretchability and required durability. Moreover, a sensing materials with zero dimension or one unit morphology is typically subject to its own structural properties and cannot be able to take both sensitivity and stretchability concurrently, this due to their low aspect rations as such they exhibited low sensitivities and sensing range [23]. For instance, Park et al. reported the fabrication of strain sensor based on silver nanoparticles thin film which is patterned on polydimethylsiloxane (PDMS); the sensor exhibited a maximum gauge factor (GF) of 2.05 at a maximum strain of 20 % [21]. Correspondingly, one-dimensional materials exhibit substantial stretchability and relatively wide strain sensing range [24].

2.2 MXene: New 2D Material

A newly ancestry of transitional metal carbide, compound of nitrogen (nitride) or carbon nitride in 2D form is called MXene. It is rich in surface functional groups with excellent ion exchange and hydrophilic properties. Due to its functional and mechanical property closeness to graphene, coupled with its unique electrochemistry, physicochemical and outstanding mechanical performance, MXene has recently attracted attention in forming functional nanocomposites by combining them with a wide range of organic and inorganic materials [25]. The innovative work done over many years on the study and development of 2D materials has contributed to the growth of MXene-related research. This surge has resulted in a constantly expanding MXene family, more fundamental science on their chemistry and physics being discovered, and many more applications being demonstrated or proposed. Researchers at Drexel University first identified MXene in 2011 as 2D transitional metal-carbides, nitrides, and carbon nitrides that were created by carefully removing out the A-group elements usually aluminum from the 3D structured MAX phase. Figure 1 highlights the group of elements of the periodic table that make up this precursor material [26]. The usual formula is M_n+1AX_n, where M stands for transitional metal (scandium, titanium, or vanadium) whereas an elements from groups 3A and 4A (like Al, Ga, Ge, or Si) is represented by A. X is either carbon or nitrogen, with n = 1, 2, and 3 [27]. Due of their high surface energy, MXenes frequently have their surfaces discontinued during the etching process with fluorine (-F), hydroxide (-OH), and oxygen (-O) groups. Consequently, MXene's final chemical formula is $M_n+1X_nT_x$, wherein T_x stands for the reactive groups [28]. MXene basically has three structures (M_2XT_x, $M_3X_2T_x$, and $M_4X_3T_x$) which are all derived from selectively etching their corresponding MAX phases [29].

A wide range of unique properties which relate to magnetic, mechanical [30], electrochemical [31], optical, electronic [32] and thermoelectric [33] properties have all been discovered from this large family of MXenes. Other beneficial characteristics include their hydrophilicity, high surface area, tunable surface chemistry and high atomic number [34]. These fascinating properties and characteristics unlock many possibilities of using MXene in various applications including sensors [35], energy storage [36] electromagnetic interference shielding [37], flame retardancy [38], biomaterial [39], 3D printing [40] to mention but a few. Among these areas of application, MXene-

based polymer nanocomposites as flexible strain sensors [41] and energy storage [42] gained much attention, and as such, the area is fast developing.

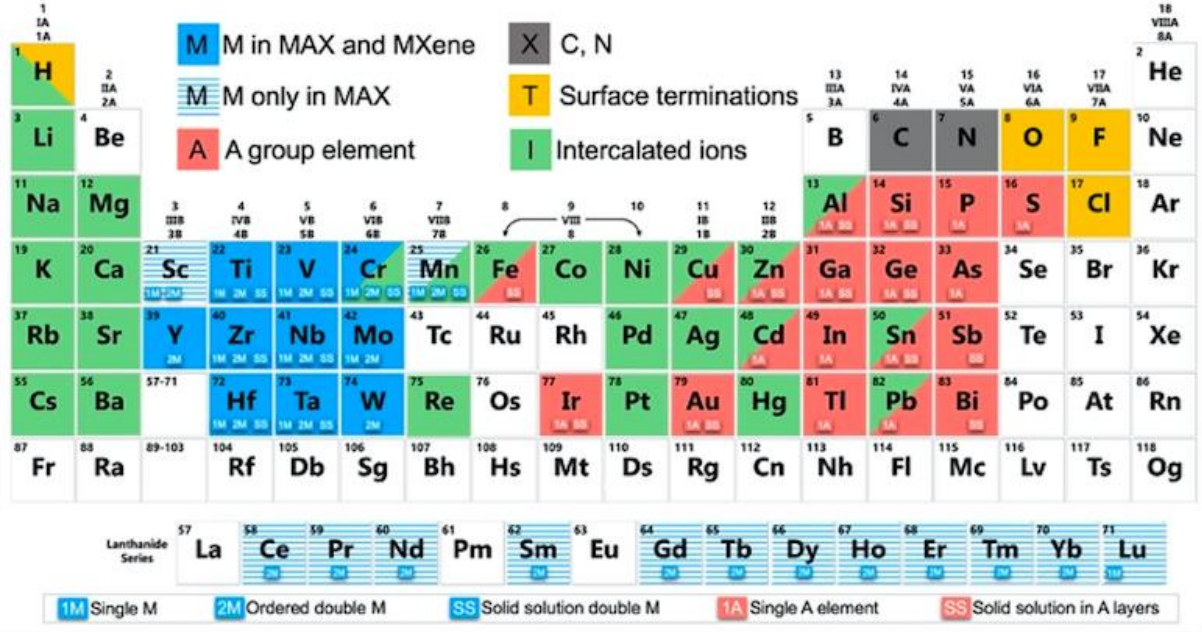

Figure 1. MAX phase and MXene production elements are shown in the periodic chart [26].

2.3 Strain Sensors based on MXene/Polymer nanocomposites

MXene /polymer flexible and stretchable strain sensor with venerable electrical conductivity and excellent mechanical properties are the cutting edge of next-generation wearable electronics and supercapacitors [43]. These sensors converted the tensile strain into electrical signals output. When an external force is applied, the internal networks of conductive material crack, causing a change in electrical properties [43]. Numerous studies have been conducted to enhance the performance matrices of flexible strain sensors based on MXene incorporated with polymer composites, including sensitivity, stretchability, and stability. For example, Lu et al. [44] demonstrated the fabrication MXene-based hydrogel flexible strain sensor. $Ti_3C_2T_X$-MXene was composited with poly (vinyl alcohol) incorporated with polyvinyl pyrrolidone (PVP) multilayered matrix hydrogels. As-fabricated sensor shows high stretchability up to 2400 %, excellent stress and toughness. This confirm the robust interaction among poly (vinyl alcohol) and its chains attractive force which endowed the hydrogel. A strain sensor [45] was prepared with micro-crack structure by applying a pre-stretching treatment to the nonwoven fabric. A sensing range of 83 % with gauge factor of 3405 and detection threshold of 0.1 % were achieved. A stable sensing behavior, short

recovery time and long-term sensing stability was displayed using different strain levels. A synthesis and crosslinked MXene (Ti_3C_2) with sodium alginate and acrylamide to fabricate a double network hydrogel flexible strain sensor [46]. The obtained strain sensor exhibited tensile properties (3150%), Young's module of 2.03 kPa^{-1}, high tensile sensitivity (GF = 18.15). Yang et al. [47] developed versatile strain sensor based on a matrix structure MXene incorporated with polyurethane mat. Figure 2 (a–d) show preparation of polyurethane/MXene strain sensor, digital image of polyurethane/MXene strain sensor, SEM micrographs of polyurethane/MXene with interconnecting structure, and shriveled structure respectively. The polyurethane mat stucture was synthesized using a simple and efficient electrospinning technology. To fabricate the strain sensor, the conducting MXene sheet was adhered to the matrix structured-P using electrostatic contact. The resultant strain sensor exhibited high sensitivity of 228, limitation of detection (0.1%) and good stability. A strain sensor [48] fabricated by modifying Ti_3C_2 MXenes and amino poly(dimethyl siloxane) using tiny biological molecules through esterification process. Due to the homogeneous dispersion of the modified MXenes, the composite exhibited good electrical conductivity, remarkable tensile characteristics, because several chemical bonds and amine bonds are reversible, high efficient self-healing can occur without the requirement for outside stimulus.

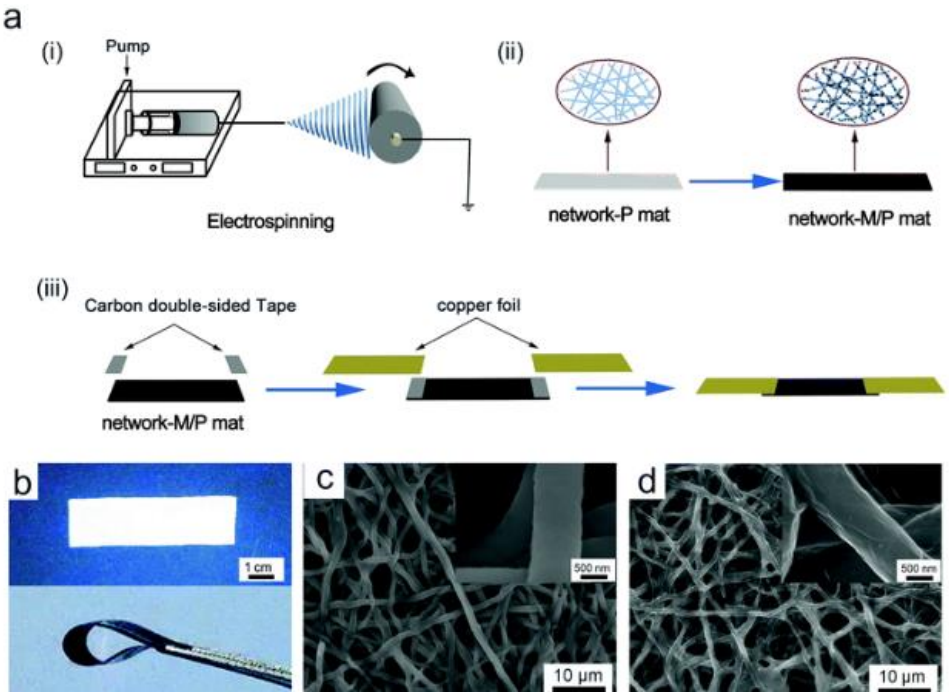

Figure 2. (a) Preparation of polyurethane/MXene strain sensor, (b) digital image of polyurethane/MXene strain sensor, (c,d) SEM micrographs of polyurethane/MXene with interconnecting structure, and shriveled structure respectively [47].

An experiment [49] demonstrated the construction of a self-healable nanostructure MXene build in with rubber based elastomer for strain sensor. Here, the MXene were modified with serine to construct bonding interface through esterification reaction. The bonding facilitated the formation of the nanostructured conductive network. The resultant MXene/rubber strain sensor showed a high sensitivity (GF= 107.43), a low limitation (0.1 %), responsiveness of 50 ms and toughness recovering of 12.34 MJ m^{-3}. Seyedin et al. [50] fabricated $Ti_3C_2T_X$-MXene/ polyurethane strain sensor by a wet-spinning technique using acetic acid and isopropanol as coagulating agents. The obtained MXene/polyurethane strain sensor displayed high electrical conductivity of MXene and satisfied stretchability of polyurethane.

Expanding the interlayer gap, conductive polymer such as polypyrrole was intercalated into multilayer or monolayer MXene nanosheets; the modified sheets produced high capacitance values and outstanding cycle performance. High performance polymer/MXene nanocomposites require the use of functional MXenes in conjunction with the polymers for further improved physical qualities [51]. In the recent years, it has proven that hybridizing nanofillers results in synergism in the desired properties of the end product. For instant, 2D nanomaterials tend to restack within the polymeric matrix due to the van der Waals forces resulted from its large surface area. Upon adding other geometrical nanofiller– such as 0D and 1 D – into polymer/2D material, it enhances the dispersion quality and enhance functional and mechanical properties of final composite materials [52]. In this paragraph, our focus is on carbon nanotubes as a synergistic 1D nanofiller for MXene since they are one of the most famous and common carbon allotropes. CNTs, which are a highly conductive 1D material, not only guarantee the flexibility of MXene sheets but also inhibit restacking and facilitate ion transport within the MXene flakes. Additionally, the insertion of CNTs to the rolled film electrodes of delaminated Ti_3C_2 MXene has demonstrated to enhance the capacitance performance in the electrolyte [53]. These features of conductive polymers and CNTs are proving to be suitable for fabricating flexible strain sensor and supercapacitors as discussed below.

Spray coating technique was employed to synthesis highly flexible strain sensor using $Ti_3C_2T_X$ MXene and CNT as conductive phase [54] (Figure 3a). Delaminated $Ti_3C_2T_X$ MXene flakes suspension was spray-coated onto the latex to formed thin continuous layer of MXene flakes, thereby drying using nitrogen gas gun. Furthermore, CNT layer was dispersed using the same

technique onto the top of the layered MXene flask. Figure 3b demonstrates the Tyndall effect of the MXene and CNT colloidal solutions, revealing their good dispersion property, which is advantageous for producing homogenous films. Additionally, Figure 3 (c, d) show the transmission electron microscope (TEM) images of MXene flake and water–soluble SWCNTs. The MXene flakes lateral dimension is varying from several millimeter to countless nanometers. Figure 3e shows the photograph of the strain sensor at resting stage and after stretching up to 100 % and 200 %. The fabricated sensor shows high GF of 772.6 (Figure 4a), high stretchability of 130 %, tunable sensing ranges from 30 % to 130 %, thin dimension of less 2 μm, and stability with 5000 cycles. Multi-cycle test in resistance variation was performed at applied strain of 5, 10, 20 and 50 % respectively (Figure 4b). Moreover, the fabricated sensor has the tendency to detect smaller as well as larger deformation with high limit of detection of 0.1% (Figure 4c). Figure 4d presents the strain sensor's equivalent resistivity performance at various frequencies.

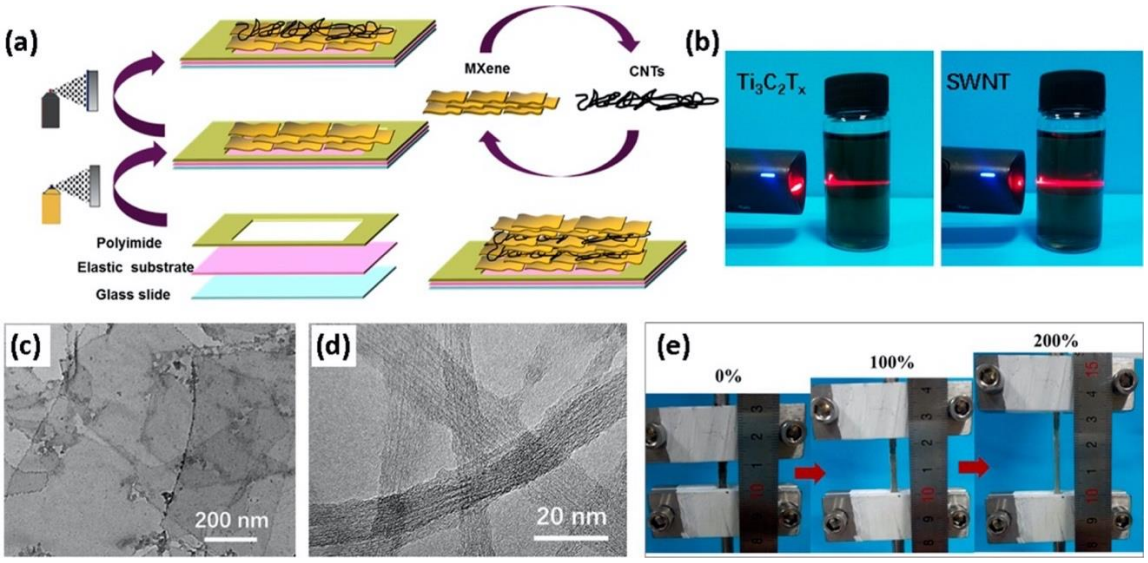

Figure 3. (a) Schematic illustrating synthesis of MXene incorporated with CNT layer; (b) Tyndall effect of MXene and SWNT suspension, (c,d) TEM images micrograph of MXene And SWNT, respectively, (e) strain sensor at different percentages [54].

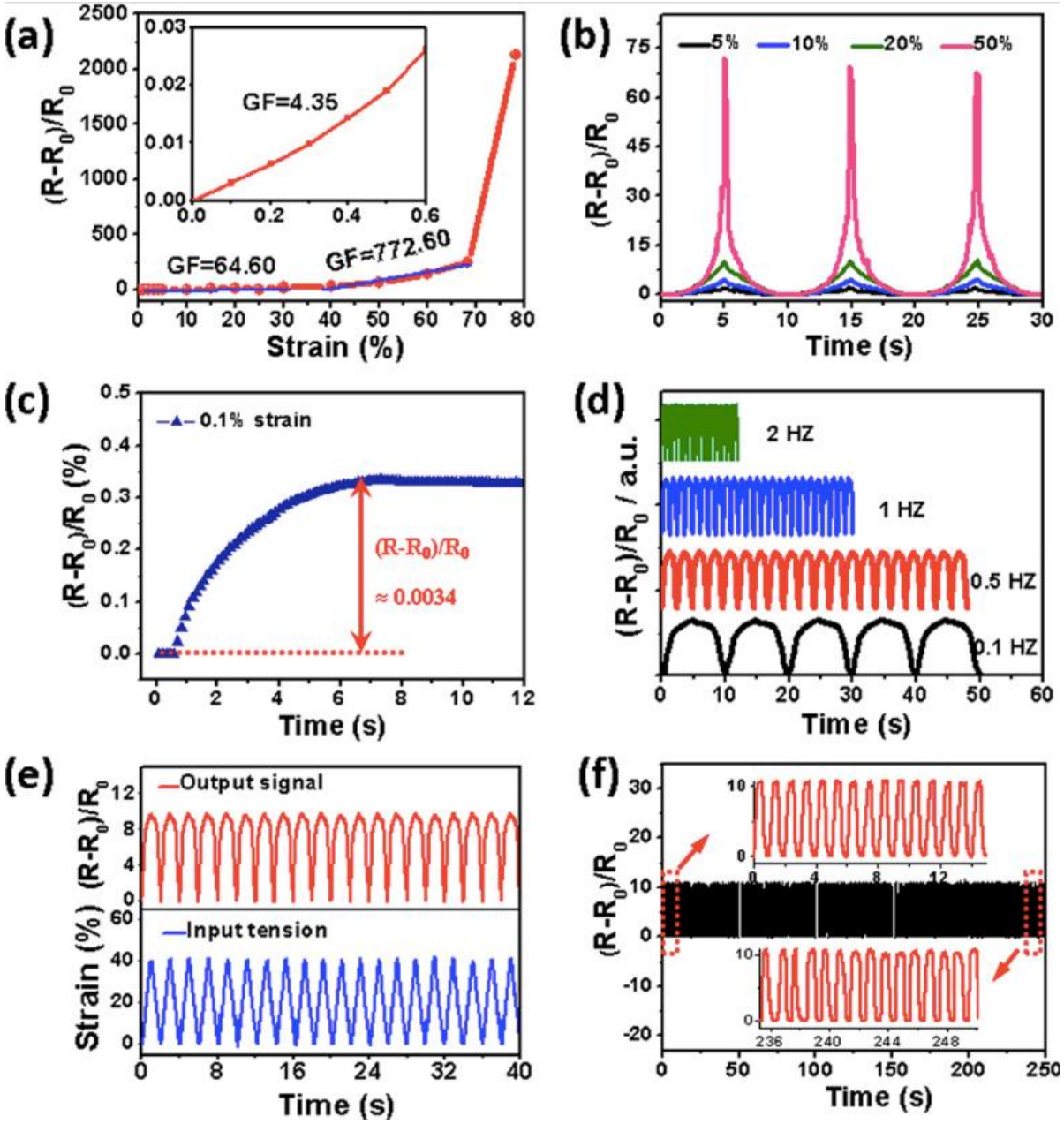

Figure 4. (a) Relative resistance-strain curve; (b) resistance variation, (c) resistance response, (d) resistance response at various frequencies, (e) resistance with strain as a function of time, (f) durability test [54].

CHAPTER 3

EXPERIMENTS AND METHODOLOGY

3.1. Materials

The Ti_3AlC_2 MAX phase powder (90%) with a particle size of ≤ 40 μm was purchased from Sigma-Aldrich Inc. (USA). The multi-walled carbon nanotube (MWCNT, >95% carbon basis) with an outer diameter of L: 10-40 nm x 0.5-1.5 mm was kindly supplied by Sigma-Aldrich Inc. (USA). Lithium fluoride (LF, 99.95% purity, size <100 μm) was provided by Nanografi Nano Technology Co., Ltd. (Turkey). Hexadecyltrimethylammonium bromide (CTAB, 98% purity) was purchased from Sigma-Aldrich Inc. (USA). Hydrochloric acid (HCl, 37%) and chloroform (99.8%, amylene stabilized) were obtained from Sigma-Aldrich Inc. (USA). Ethanol (99.9 GC) was also purchased from Sigma-Aldrich Inc. (USA). Ecoflex 00-50 MRW 1A:1B was supplied by Smooth-on Co. (USA). The filter membrane (0.45 μm diameter, 47 mm) was purchased from Whatman, plc. (UK).

3.2. Synthesis of MXene

MXene was synthesised using fluoride-based salt etchant [55]. Briefly, 1 g of LiF was added into 10 mL of HCl and continuously stirring until was completely dissolved. A total of 1 g Ti_3AlC_2 MXene-precursor powder was slowly added over a period of 5 min. The reaction was allowed to run under continuous magnetic stirring for 24 h at room temperature. Then, the acidic mixture was washed with distilled water through centrifugation technique using 50 mL centrifuge tube at 3500 rpm. The washing process was continued till reaching pH value between 4–5. The colloidal suspension was filtered and dried in a fan oven overnight at 60 °C. Figure 5 present the schematic representation of MXene synthesis.

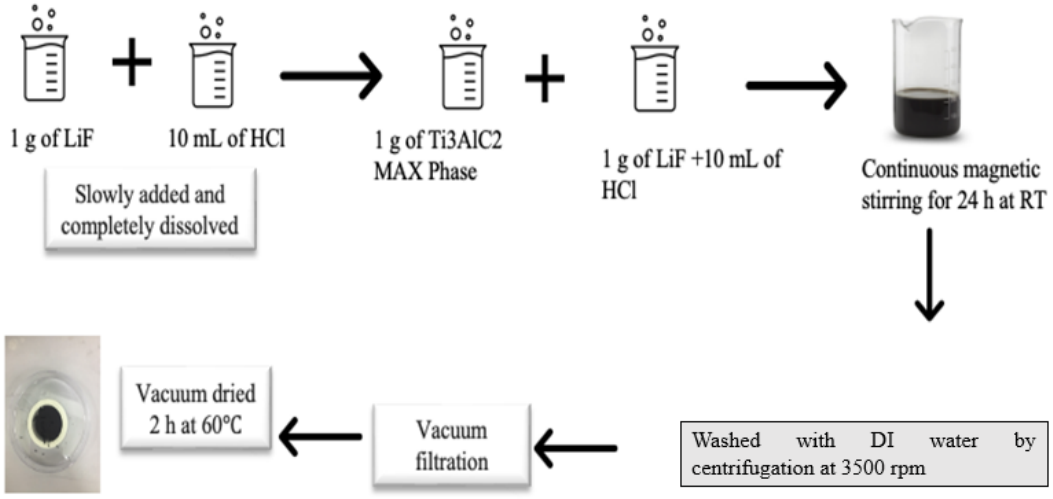

Figure 5. Schematic representation of MXene synthesis.

3.3. Modification of MWCNTs and preparation of $Ti_3C_2T_x$-MXene/m-MWCNTs

MWCNT was modified using CTAB [56]. 0.7 g of CTAB was dissolved in 10 mL of distilled water. Then, 1 g of MWCNTs was added to the mixture. The mixture was sonicated in a water bath for 1 h below room temperature to produce modified m-MWCNTs. The resulting mixture was then filtered and vacuum-dried for 2 h at 60 °C. Figure 6 displays a schematic representation of the modification of MWCNTs.

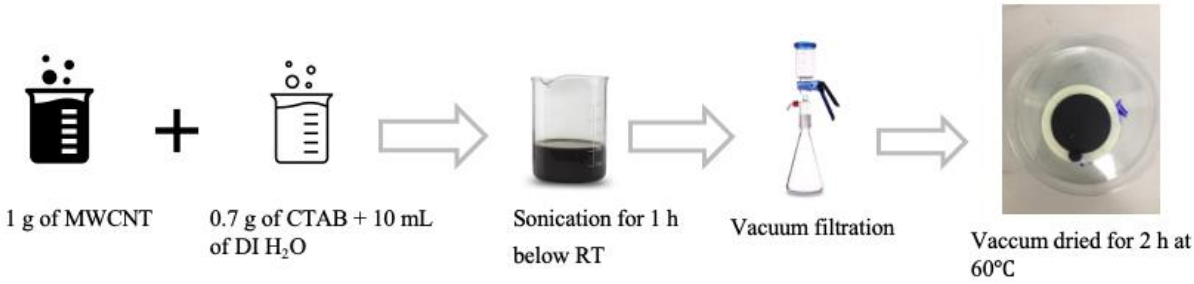

Figure 6. Representation of modification of MWCNTs.

Firstly, m-MWCNTs suspension was prepared by dispersion into CTAB solution (mass ratio 2:1). The solution was sonicated for 1 h. Then, MXene solution was prepared by dispersing MXene powder into 10 mL of deionized water and sonicated for 1 h. The m-MWCNTs suspension and MXene solution was mixed and sonicated for 1 h together with in different weight ratio (1:1, 2:1, 1:2). Figure 7 presented the schematic diagram of preparation of MXene/m-MWCNTs.

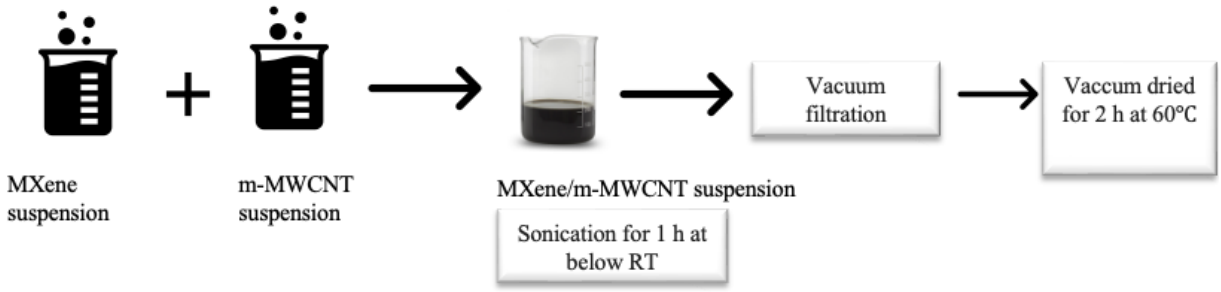

Figure 7.Schematic representation of preparation of MXene/m-MWCNTs composite.

3.4. Fabrications of m-MWCNT/MXene/Ecoflex composite strain sensor.

Strain sensor was fabricated by direct deposition method (Figure 8). Firstly, sample A was fabricated by using MXene and Ecoflex only. The two parts (A and B) of Ecoflex were mixed together in a 1:1 mass ratio, with a total mass of 10 g, and stirred for 5 min. Then, 0.4 g of MXene were directly dispersed into the Ecoflex mixture and stirred well for approximately 10 min until fully homogenized. Air bubbles were removed by placing the solution in vacuum until the solution was fully degassed (10 min). At this stage, two methods were used. One method involved using a mold with dimensions of 3 cm × 1.5 cm × 2 cm to pour the solution into the mold, while wire electrodes were attached to both sides. The composite was left for 4 h at room temperature until it was fully cured and then peeled off from the mold. The thickness of the sample is 0.13 mm. The second approach is using slurry cast method. The composite was poured onto a casting glass, and a doctor blade was used to spread it and form a film. The prepared composite was then left to cure at room temperature for 4 h until fully cured. The desired size was cut, and wire electrodes were attached to both sides with the help of silver paste. Similar approach was used to prepare Ecoflex/ MXene/MWCNT composite. For the preparation of MXene/m-MWCNTs/Ecoflex, 0.3 g of both

MXene and m-MWCNTs were used to prepare the composite. Whereas, the two parts (A and B) of Ecoflex were mixed together in a 1:1 mass ratio, with a total mass of 10 g.

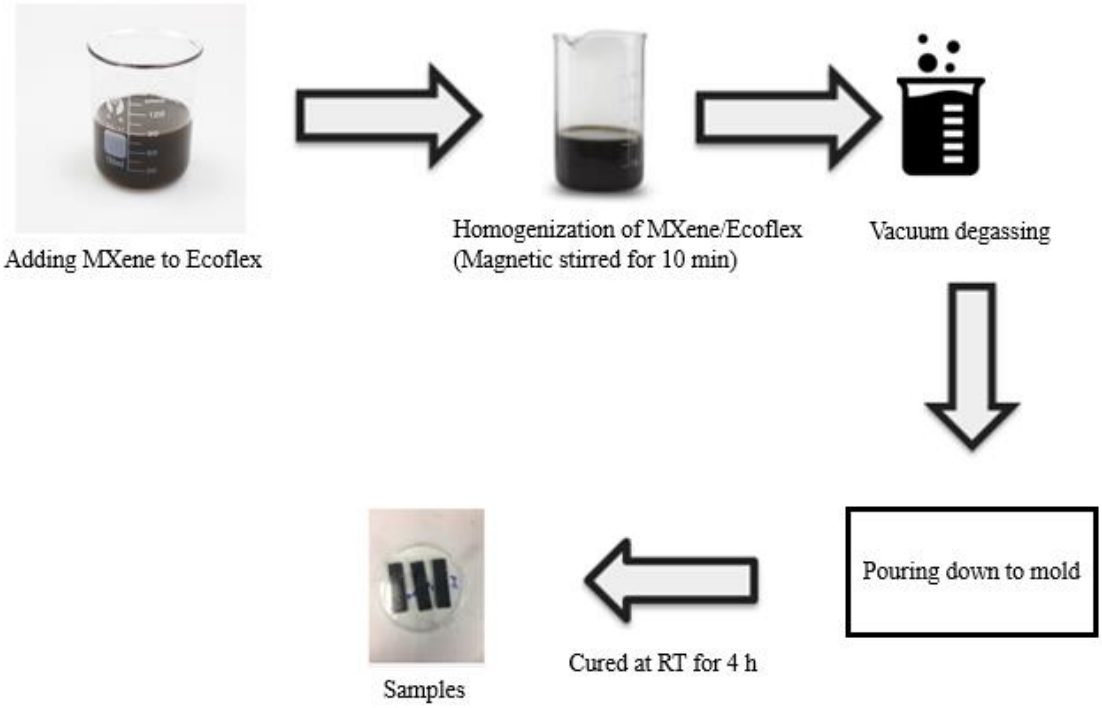

Figure 8. Fabrication of a strain sensor sample using m-MWCNT/Ecoflex.

CHAPTER 4

RESULTS AND DISCUSSION

4.1 Chemical morphology and microstructure

The X-ray diffraction (XRD) technique was employed to analyze the crystal structure of the MXene and MWCNTs. The XRD measurements were conducted using a Rigaku Smart lab XRD machine, as shown in Figure 9a, the X-ray diffraction patterns for MXene, MWCNTs, and m-MWCNTs. The MXene sample demonstrates a diffraction peak at a 2θ value of 18.5, which is attributed to the spatial distance between its basal planes in the (002) crystallographic orientation. Both the MWCNTs and m-MWCNTs exhibit distinctive diffraction patterns at a 2θ value of 26, which can be attributed to the presence of carbon atoms in the (002) plane [57]. MXene/m-MWCNT shows small peak at 29.8°. The primary bonding mechanism in the MXene/m-MWCNTs composite is attributed to the carbon structure derived from the modified MWCNTs. The significant reduction in C-Ti-O bonds serves as confirmation that the MWCNTs have been fully incorporated into the MXene, while the majority of the chemical structure of the MXene sheet remains unchanged [57]. The chemical functional groups of MXene and multi-walled carbon nanotubes were examined and identified using Fourier transform infrared (FTIR) spectroscopy. In Figure 9b, by analyzing the FTIR spectra, it was discovered that MXene exhibited two specific bands at 3365 cm^{-1} and 1620 cm^{-1}, which are indicative of the presence of -OH and -C=O functional groups, respectively. MWCNT displayed bands at 3450 cm^{-1} and 1520 cm^{-1}. Morphology of the MWCNT and MXene were studied using scanning electron microscope (SEM) JSM-IT200 (LA). Figure 10a shows micrograph of the MAX phase powder. In Figure 10b, SEM micrograph of synthesized MXene presented in layered structure confirming that Al element layer was successfully removed from MAX phase. In Figure 10c, shows SEM image of MWCNTs confirming that the structure is in sponge like material. Figure 10d displays an SEM image of m-MWCNTs with traces of CTAB, showing full subjugation. Concurrently, Figure 10e shows an SEM image of MXene/m-MWCNTs, revealing complete coverage and bonding of MXene into m-MWCNTs.

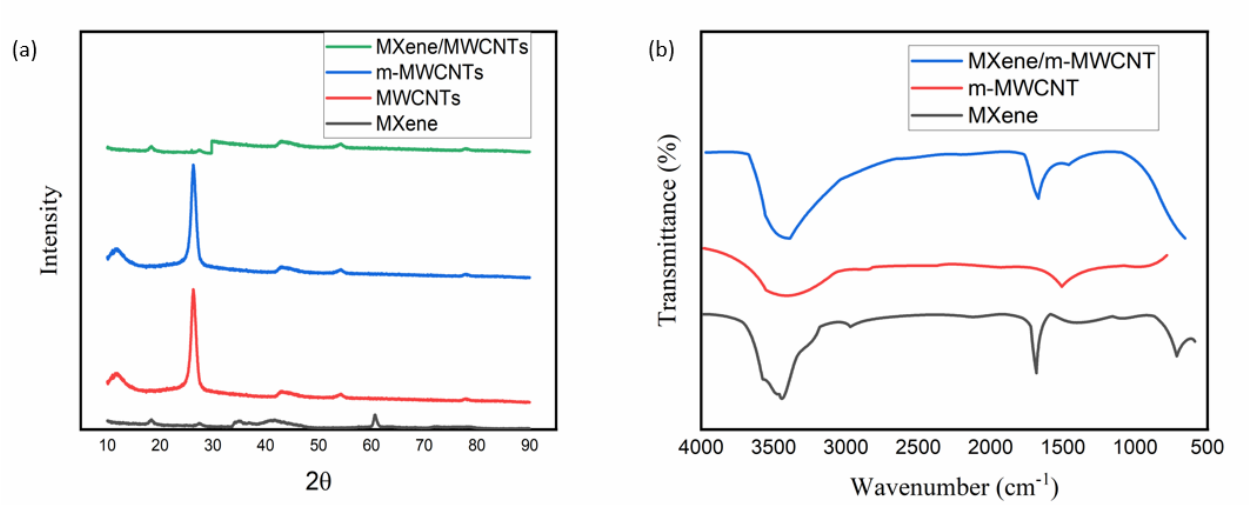

Figure 9. (a) XRD pattern of MXene, MWCNT and MXene/MWCNT, (b) FTIR Spectra of MXene, MWCNT and MXene/MWCNT.

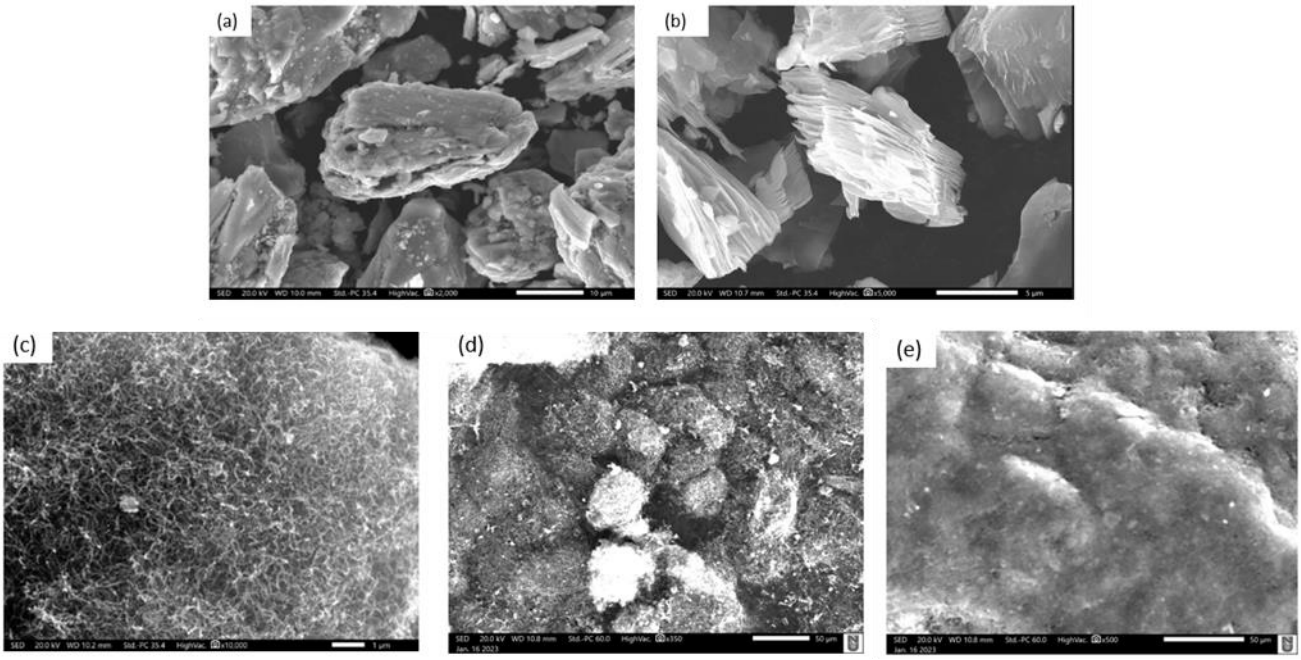

Figure 10. SEM images: (a) MAX phase powder; (b) MXene nanosheet, (c) MWCNT, (d) m-MWCNT, (f) MXene/MWCNT.

4.2. Mechanical measurements

In order to study the mechanical strength, three sample were prepare in this order; Ecoflex only, MXene/Ecoflex, and MXene/m-MWCNT/Ecoflex. The test was carried out using universal tensile testing machine as shown in setup in Figure 11.

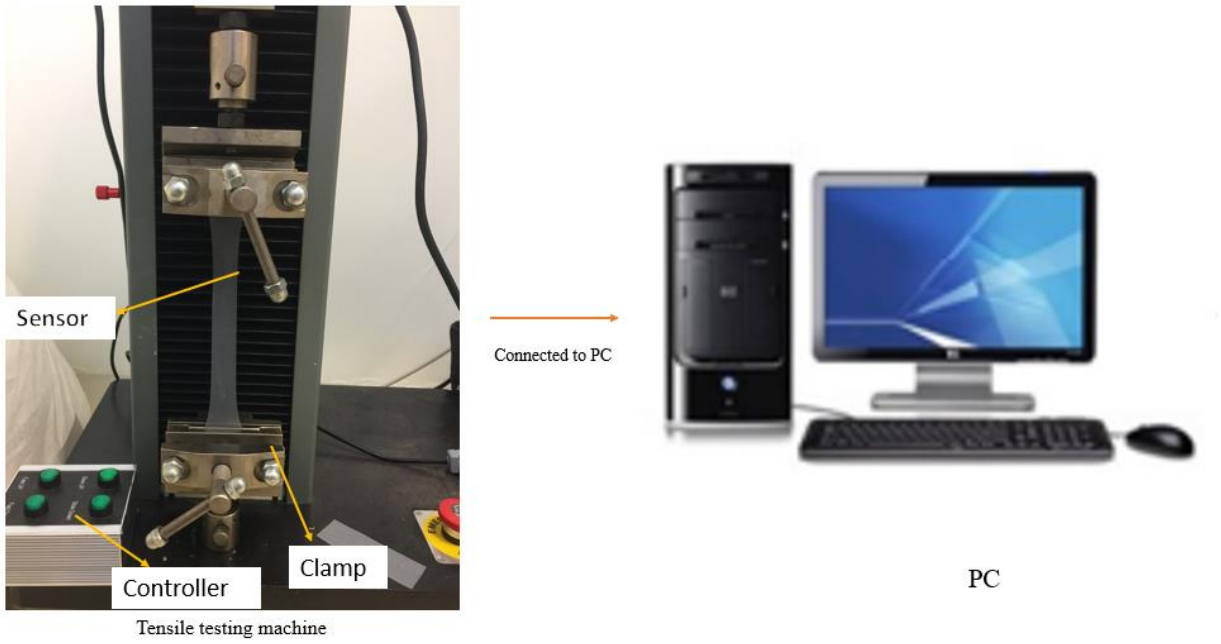

Figure 11. Mechanical measurement setup.

The relationship between stress and strain within the elastic region can be described as nearly linear. As shown in Figure 12**,** the combination of MXene/m-MWCNT and MXene demonstrates excellent mechanical strength compared to pure Ecoflex. The MXene/m-MWCNTs recorded a tensile strength of 16 MPa, slightly higher than MXene at 15.4 MPa, while pure Ecoflex exhibited a tensile strength of 9.7 MPa. Furthermore, the breaking load of the MXene/m-MWCNTs composite was measured at 280 N. This suggests that the breaking load and elongation increase as the content of MXene/m-MWCNT increases, until the amount reaches a certain destructive level of the Ecoflex. The significant enhancement in tensile stress and strain is attributed to the MXene structure and the effective integration of m-MWCNTs. Although m-MWCNTs generate frictional force that could potentially hinder tensile strength, the layered structure of MXene promotes an increase in surface contact area between layers, which helps to enhance the tensile properties.

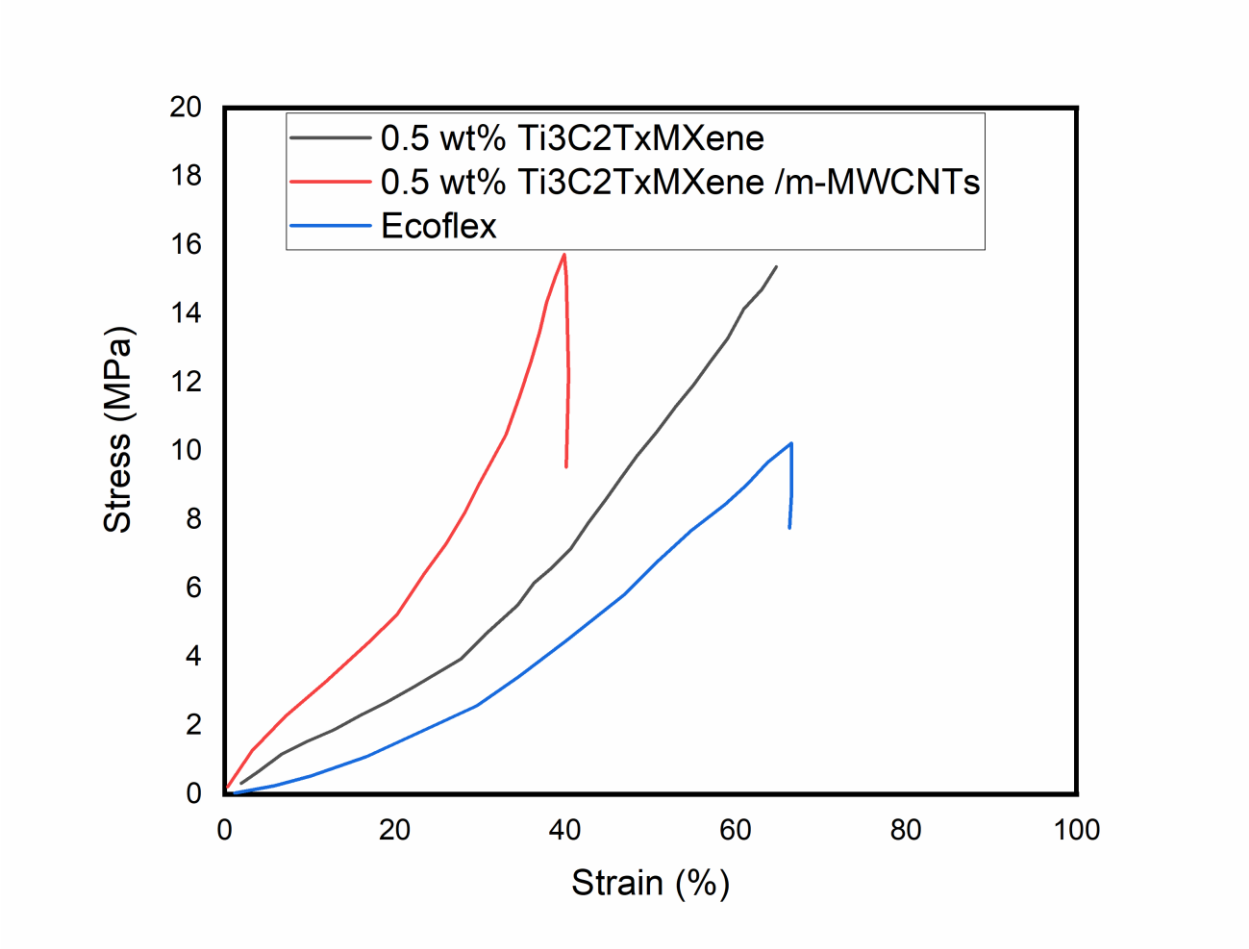

Figure 12. Mechanical properties of MXene/m-MWCNT/Ecoflex: tensile strength.

4.3. Electromechanical performance of MXene-based composites

The resistance of a strain sensor refers to how easily electrical current flows through its conductive component when it is subjected to strain. When a strain sensor is stretched or compressed, its conductive element experiences a change in resistance, which can be measured and used to determine the degree of strain or deformation that the material or structure is undergoing. The gauge factor (GF) defines the sensitivity of a strain sensor, and it can be determined using the following equation:

$$GF = \frac{\frac{\Delta R}{R_O}}{\varepsilon}$$

$$\varepsilon = \frac{\Delta L}{L_o}$$

Where ΔR represents the change in resistance from R_o to R due to deformation; R_o and R are the initial and final resistances, respectively. The value ε denotes the applied strain; ΔL represents the variation in the length of the material upon a strain; and L_o represents the initial or original length of a material.

The testing setup is shown in Figure 13. The strain sensor was clamped between the stationary bar and horizontal movable part of the linear motor device. The linear motor was connected to the PC and manipulated using LinMot application software. The two electrode wires of the strain sensor was then connected to Keithley source meter integrated with triple power source. The resistivity change was recorded using KickStart application software.

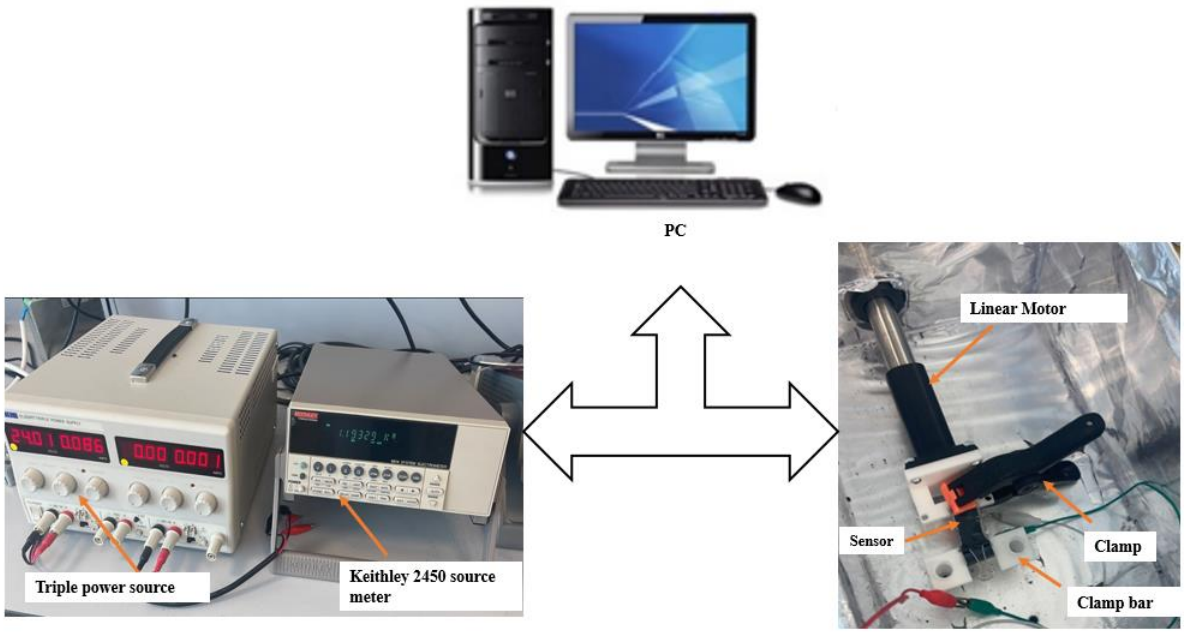

Figure 13. Electromechanical station to test strain sensitivity of Ecoflex/MXene/MWCNTs composite.

To study the sensitivity and stretchability performance of the MXene and m-MWCNTs strain sensor, two different sample with (MXene, and MXene /m-MWCNTs) were fabricated and tested within strain range of 0-60% as shown in Figure 14. The resistance-strain curve of the MXene/m-MWCNTs strain sensor indicates that it possesses a wide and adjustable range of sensitivity with

gauge factor (GF) of 7. This range can be modified by varying the concentration and weight percentage of both the MXene and m-MWCNTs employed in the sensor. Similarly, Table 1 presents strain sensor made for different material with their gauge factor as compared to this work. For sample with MXene only, the gauge factor (GF) is calculated to be at 3.87.

There are various reasons for the variation in gauge factor observed between MWCNT and MXene-based strain sensors. A notable explanation is the higher aspect ratio of MWCNTs relative to MXenes. This aspect facilitates their alignment with the direction of the applied strain, causing a more pronounced change in electrical resistance per unit strain, ultimately resulting in a higher gauge factor. Also, the mechanical characteristics of MWCNTs and MXenes are responsible for the variation in GF observed in strain sensors produced from these materials. MWCNTs exhibit a higher Young's modulus, enabling them to withstand greater strains without breaking. In contrast, MXenes are more prone to cracking under strain due to their brittle nature, which can have a detrimental effect on the performance of the strain sensor. Additionally, the electrical conductivity of MWCNTs exceeds that of MXenes, resulting in reduced electrical noise and enhanced detection of changes in electrical resistance. This ultimately yields a higher GF.

Additionally, MXene/MWCNT based strain sensors demonstrate a higher GF compared to MXene-based ones due to MWCNTs' greater aspect ratio, improved mechanical properties, and higher electrical conductivity.

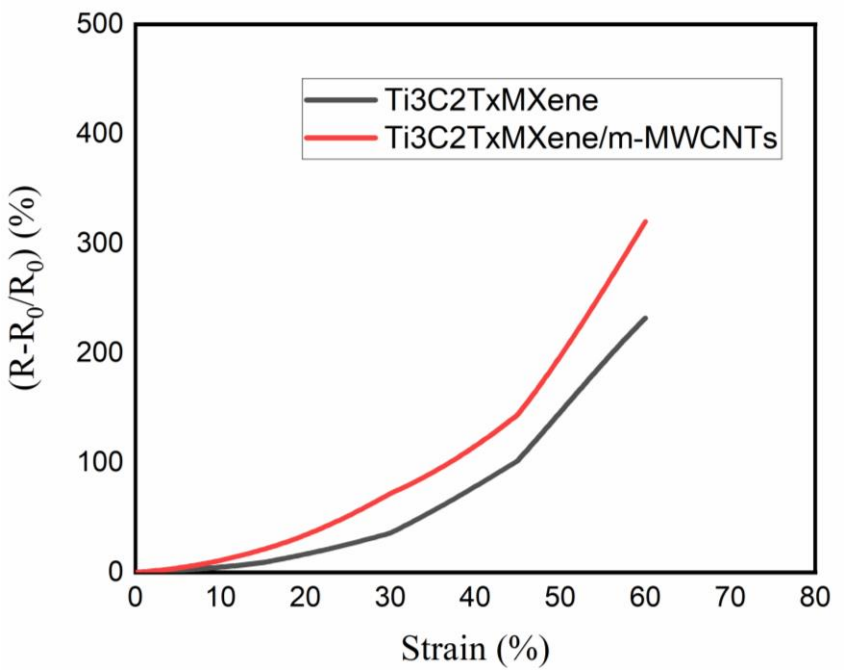

Figure 14. Relative resistance-strain curve within 0-60% strain of MXene, and MXene/m-MWCNTs.

Table 1.comparison of strain sensor made from different materials

Material Used	Gauge Factor (GF)	Ref
Air-laid paper/MXene	1-2.58	[58]
MXene/Polyaniline	46	[59]
Chitason/Polyacrylamide hydrogel based	1.65	[60]
PDMS Supramolecular/MXene	3.6	[48]
Polyethylene/MWCNT	7.6	[61]
Polyurethane/MWCNT	7	[62]
Ecoflex/AgNWs	0.7	[63]
Paper/MXene	17.4	[64]
Cotton fabric/MXene	4.11	[65]
Coated-MXene/cotton fabric	7.6	[66]
MXene/nanowires	5.2	[67]
MXene /m-MWCNTs	7	This work

Figure 15a show MXene /m-MWCNTs strain sensor stretched at 10% strain with different frequencies (0.01 Hz, 0.05 Hz, 0.1 Hz, 0.2 Hz and 1 Hz). The strain sensor seems to be able to maintain stability and respond dynamically to changes in frequency, as shown by the results presented by the data graph. This might come as a result of the Ecoflex, m-MWCNTs, and MXene having a strong bonding. Thus, the amplitude modulation of the electrical signal was nearly proportional to the increase in frequency. In Figure 15b, the MXene/m-MWCNT strain sensor was tested for changes in relative resistance under a 30% with frequency of 1 Hz strain at displacement rates of 0.0025 m/s, 0.005 m/s, and 0.007 m/s. It was found that as the rate of displacement increased, a stable and uniform peak value was detected. This suggests that the sensor's response remained constant regardless of the change in displacement. Strain values of 15%, 30%, and 45% were used to demonstrate the frequency response as shown in Figure 15c, indicating that the sensor's response to the cyclic tensile test was dependable and consistent, the response as well as recovery of each signal tested had comparable shapes and magnitudes.

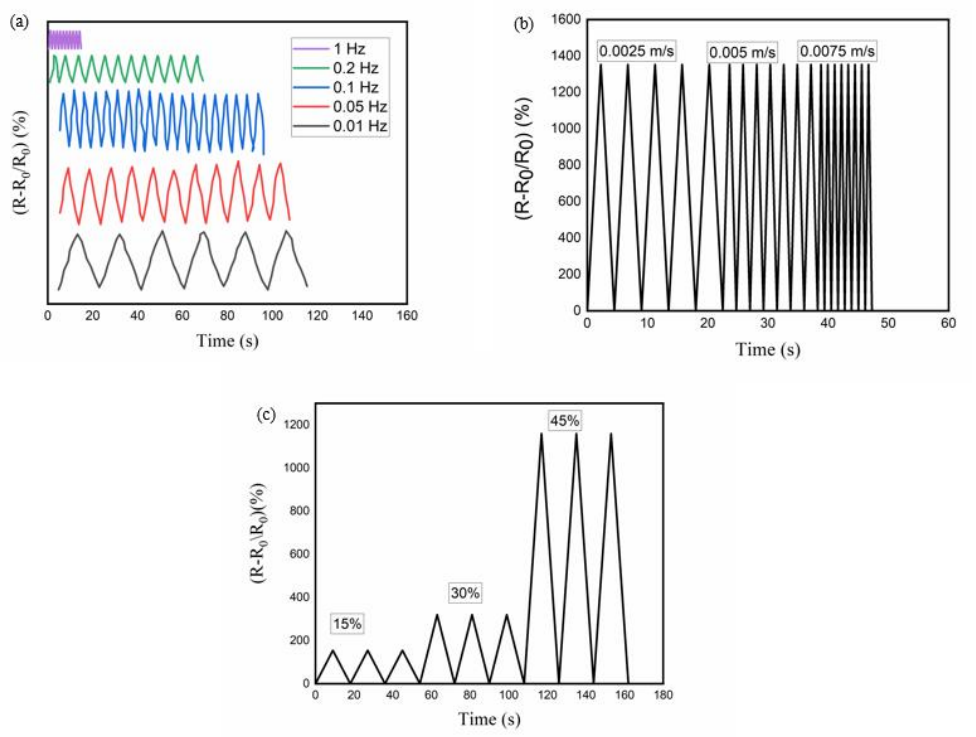

Figure 15. (a) MXene /m-MWCNTs strain sensor stretched at 10% strain with different frequencies (0.01 Hz, 0.05 Hz, 0.1 Hz, 0.2 Hz, and 1 Hz); (b) MXene /m-MWCNTs strain sensor stretched at 30% strain with different displacement rate (0.0025 m/s, 0.005 m/s, and 7 m/s), (c) MXene /m-MWCNTs strain sensor stretched at 15%, 30% and 45% strain.

To assess the durability and electromechanical response of the MXene/m-MWCNTs strain sensor, we obtained data by subjecting it to 10% strain for 1000 stretching and releasing cycles at a frequency of 1 Hz. The magnified insets in Figure 16 show the first 5 cycles, 5 cycles in the middle, and the last 5 cycles. The resistance remained constant with good reproducibility during the first 5 cycles, indicating excellent fatigue resistance of the sensor. Similarly, the sensor displayed nearly identical sensing signals during the 5 cycles in the middle and the last 5 cycles, suggesting that it can withstand fatigue, making it suitable for wearable device applications.

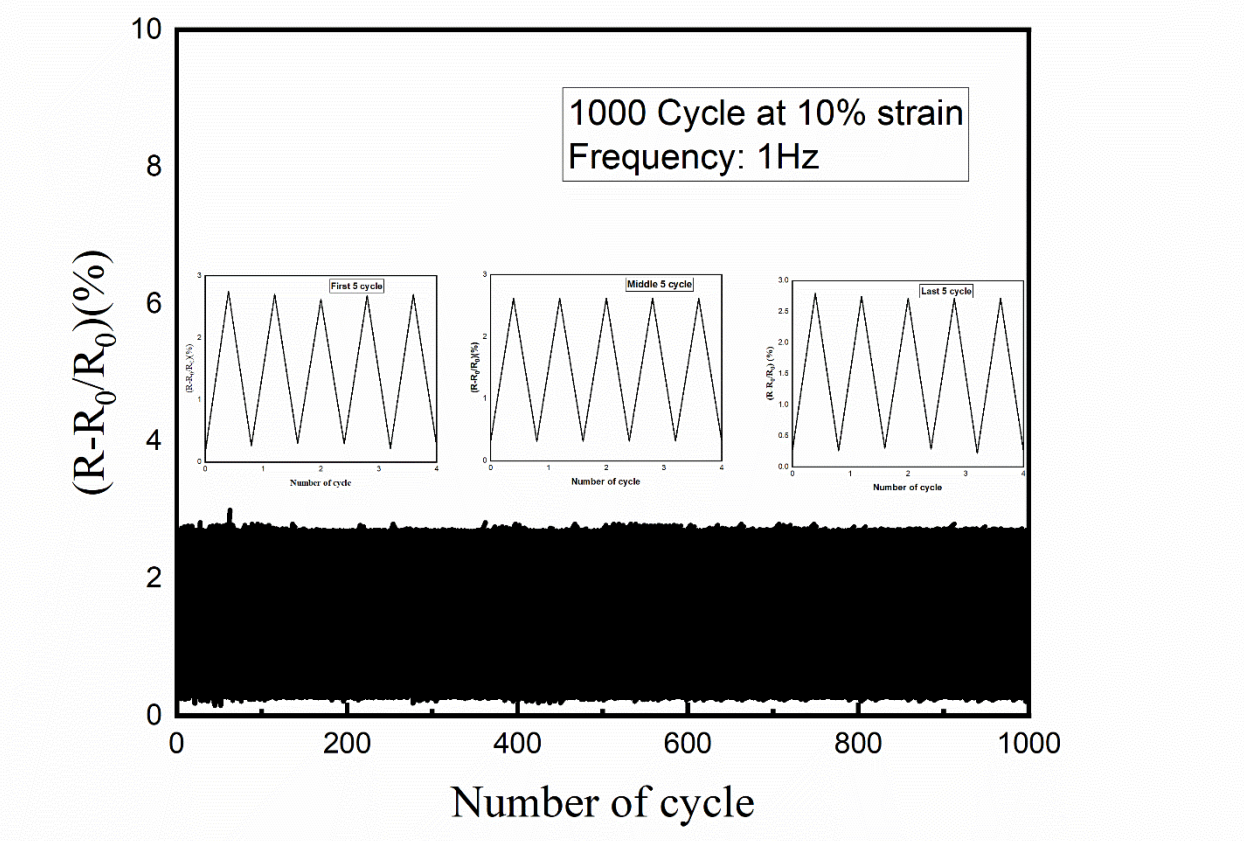

Figure 16. Cyclic tensile test for MXene/m-MWCNTs strain sensor at 10 % strain.

4.4. Real-Time Application human movement

The MXene/m-MWCNTs strain sensor exhibits excellent sensing performance, including good sensitivity, a wide sensing range, an extremely quick response, and outstanding cycle stability. This makes it possible to utilize the sensor as a wearable device to instantaneously monitor various motions of the human body. For instance, Figure 17a, b shows digital photograph of finger bending and the variations in electrical signals produced by the finger-mounted MXene/m-MWCNTs strain

sensor. When the finger is bent, the resistance of our MXene/m-MWCNTs sensor rises sharply and instantly. Once the joint is relaxed, the sensor's resistance returns to its initial value, demonstrating its efficiency in tracking various human movements. Moreover, when the sensor was mounted on the hand, wrist, and knee joints, it immediately displayed reliable electrical signals for bending motions of the joints as shown in Figure 17c, d, e and f, with respective digital photographs. This demonstrates the enormous potential of the MXene/m-MWCNTs sensor for use in assessing human health.

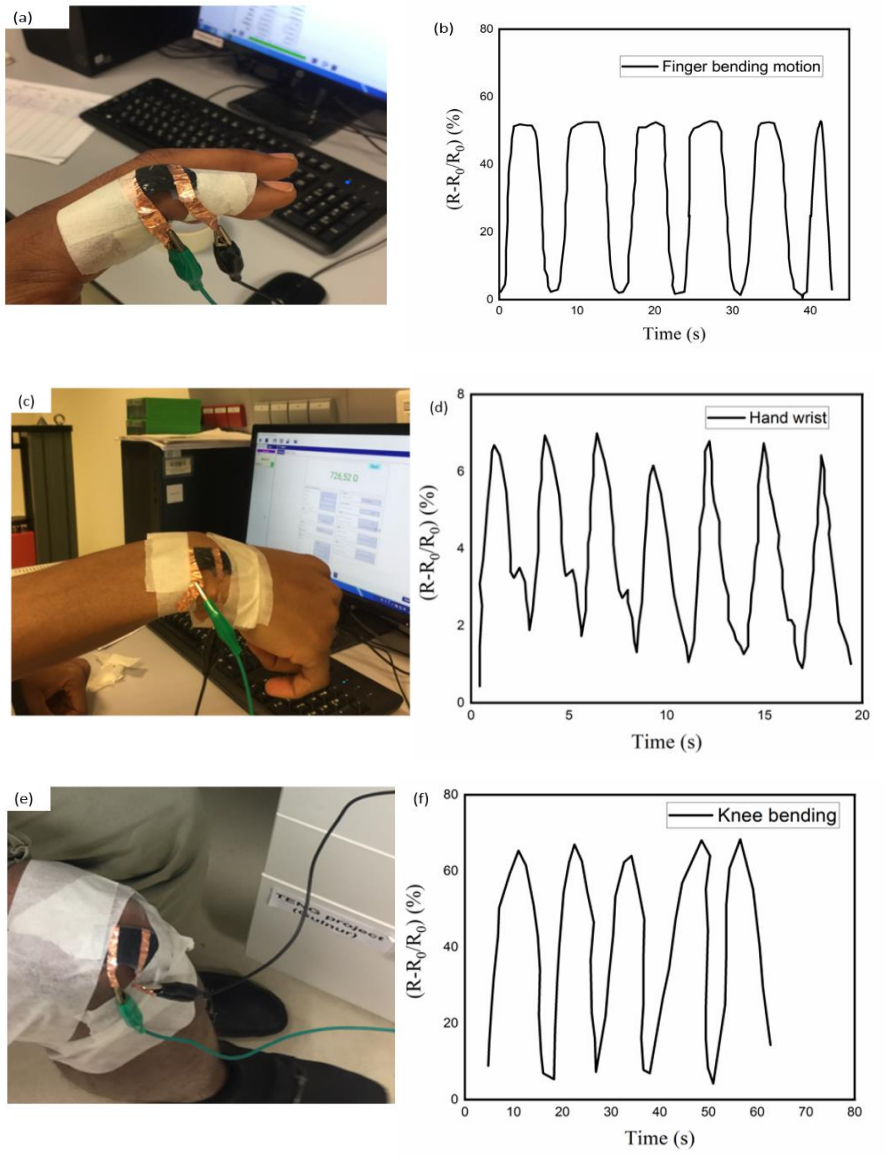

Figure 17. Detecting human body motion using MXene /m-MWCNTs strain sensor: (a) Digital photograph of finger bending; (b) finger bending graph, (c) Digital photograph of hand wrist motion, (d) Hand wrist motion graph, (e) Digital photograph of Knee bending movement, (f) Knee bending graph.

CHAPTER 5

Conclusions

A flexible strain sensor was constructed using conductive materials and elastomers. Firstly, general concept of sensors has been studied and presented. Sensors can be categorized based on their characteristics, materials being used or measured (physical and chemical), and can also be categorized as active or passive. Literature review was conducted and presented the approaches of fabrication of flexible strain sensor using different conductive materials. Moreover, in the experimental part we synthesized MXene using chemical etching approach to etch Al element layer from the MAX phase powder. Chemical morphology and microstructure of MXene sheets were examined using SEM, XRD, and FTIR. MWCNTs was modified by using CTAB in order to have good electrostatic bonding between MWCNTs and MXene. Samples with different mass contents (MXene, and MXene /m-MWCNTs) were fabricated and mechanically tested; MXene/m-MWCNT recorded a tensile strength of 16 MPa. The strain sensitivity of Ecoflex/MXene composites was tested within strain range of 0-60%. The sensitivities (gauge factors) were found to be 3.87 for MXene, and 5.33 for MXene /m-MWCNTs. Additionally, MXene/m-MWCNTs strain sensor underwent 1000 stretching and releasing cycles at 10% strain. The sensor exhibited consistent performance. Moreover, examine the real-time application of the fabricated sensor, the motion of different part of human body were tested and excellent response were recorded.

Reference

[1] J. Fraden, "Handbook of modern sensors: physics, designs, and applications," ed: American Association of Physics Teachers, 1998.

[2] J. Vetelino and A. Reghu, *Introduction to sensors*. CRC press, 2017.

[3] A. A. Ensafi and A. Kazemzadeh, "Optical pH sensor based on chemical modification of polymer film," *Microchemical journal*, vol. 63, no. 3, pp. 381-388, 1999.

[4] T. Yang, X. Zhao, Y. He, and H. Zhu, "Graphene-based sensors," in *Graphene*: Elsevier, 2018, pp. 157-174.

[5] P. Gründler, *Chemical sensors: an introduction for scientists and engineers*. Springer Science & Business Media, 2007.

[6] J. Janata, *Principles of chemical sensors*. Springer Science & Business Media, 2010.

[7] S. Soloman, Sensors Handbook. McGraw-Hill, 1999.

[8] W. Liu, C. Lu, X. Wang, R. Y. Tay, and B. K. Tay, "High-Performance Microsupercapacitors Based on Two-Dimensional Graphene/Manganese Dioxide/Silver Nanowire Ternary Hybrid Film," *ACS Nano,* vol. 9, no. 2, pp. 1528-1542, 2015/02/24 2015, doi: 10.1021/nn5060442.

[9] Y. Cheng, R. Wang, J. Sun, and L. Gao, "Highly Conductive and Ultrastretchable Electric Circuits from Covered Yarns and Silver Nanowires," *ACS Nano,* vol. 9, no. 4, pp. 3887-3895, 2015/04/28 2015, doi: 10.1021/nn5070937.

[10] D. Rus and M. T. Tolley, "Design, fabrication and control of soft robots," *Nature,* vol. 521, no. 7553, pp. 467-475, 2015/05/01 2015, doi: 10.1038/nature14543.

[11] Y. Ma, Y. Gao, L. Liu, X. Ren, and G. Gao, "Skin-Contactable and Antifreezing Strain Sensors Based on Bilayer Hydrogels," *Chemistry of Materials,* vol. 32, no. 20, pp. 8938-8946, 2020/10/27 2020, doi: 10.1021/acs.chemmater.0c02919.

[12] T. Purkait, G. Singh, D. Kumar, M. Singh, and R. S. Dey, "High-performance flexible supercapacitors based on electrochemically tailored three-dimensional reduced graphene oxide networks," *Scientific Reports,* vol. 8, no. 1, p. 640, 2018/01/12 2018, doi: 10.1038/s41598-017-18593-3.

[13] Q. Liu, J. Chen, Y. Li, and G. Shi, "High-Performance Strain Sensors with Fish-Scale-Like Graphene-Sensing Layers for Full-Range Detection of Human Motions," *ACS Nano,* vol. 10, no. 8, pp. 7901-7906, 2016/08/23 2016, doi: 10.1021/acsnano.6b03813.

[14] S. Li *et al.*, "Recent Advances of Carbon-Based Flexible Strain Sensors in Physiological Signal Monitoring," *ACS Applied Electronic Materials,* vol. 2, no. 8, pp. 2282-2300, 2020/08/25 2020, doi: 10.1021/acsaelm.0c00292.

[15] S. Lim *et al.*, "Transparent and Stretchable Interactive Human Machine Interface Based on Patterned Graphene Heterostructures," *Advanced Functional Materials,* vol. 25, no. 3, pp. 375-383, 2015, doi: https://doi.org/10.1002/adfm.201402987.

[16] J. Du *et al.*, "Optimized CNT-PDMS Flexible Composite for Attachable Health-Care Device," *Sensors,* vol. 20, no. 16, p. 4523, 2020. [Online]. Available: https://www.mdpi.com/1424-8220/20/16/4523.

[17] Z. Liu *et al.*, "Functionalized Fiber-Based Strain Sensors: Pathway to Next-Generation Wearable Electronics," *Nano-Micro Letters,* vol. 14, no. 1, p. 61, 2022/02/15 2022, doi: 10.1007/s40820-022-00806-8.

[18] Z. He *et al.*, "Highly stretchable multi-walled carbon nanotube/thermoplastic polyurethane composite fibers for ultrasensitive, wearable strain sensors," *Nanoscale*, 10.1039/C9NR01005J vol. 11, no. 13, pp. 5884-5890, 2019, doi: 10.1039/C9NR01005J.
[19] Z. Zhang *et al.*, "Effect of Carbon Black on the Strain Sensing Property of 3D Printed Conductive Polymer Composites," *Applied Composite Materials*, vol. 29, no. 3, pp. 1235-1248, 2022/06/01 2022, doi: 10.1007/s10443-022-10017-4.
[20] S.-H. Ha and J.-M. Kim, "Highly sensitive and stretchable strain sensor based on self-aligned and periodic cracking of wavy metal nanowire/elastomer composite film," *Smart Materials and Structures*, vol. 30, no. 6, p. 065022, 2021/05/13 2021, doi: 10.1088/1361-665x/abfb82.
[21] J. Lee *et al.*, "A stretchable strain sensor based on a metal nanoparticle thin film for human motion detection," *Nanoscale*, 10.1039/C4NR03295K vol. 6, no. 20, pp. 11932-11939, 2014, doi: 10.1039/C4NR03295K.
[22] X. Liu *et al.*, "A highly sensitive graphene woven fabric strain sensor for wearable wireless musical instruments," *Materials Horizons*, 10.1039/C7MH00104E vol. 4, no. 3, pp. 477-486, 2017, doi: 10.1039/C7MH00104E.
[23] R. Nur, N. Matsuhisa, Z. Jiang, M. O. G. Nayeem, T. Yokota, and T. Someya, "A Highly Sensitive Capacitive-type Strain Sensor Using Wrinkled Ultrathin Gold Films," *Nano Letters*, vol. 18, no. 9, pp. 5610-5617, 2018/09/12 2018, doi: 10.1021/acs.nanolett.8b02088.
[24] J. Oh *et al.*, "Pressure Insensitive Strain Sensor with Facile Solution-Based Process for Tactile Sensing Applications," *ACS Nano*, vol. 12, no. 8, pp. 7546-7553, 2018/08/28 2018, doi: 10.1021/acsnano.8b03488.
[25] M. Aakyiir *et al.*, "Elastomer nanocomposites containing MXene for mechanical robustness and electrical and thermal conductivity," *Nanotechnology*, vol. 31, no. 31, p. 315715, 2020/05/20 2020, doi: 10.1088/1361-6528/ab88eb.
[26] Y. Gogotsi and B. Anasori, "The Rise of MXenes," *ACS Nano*, vol. 13, no. 8, pp. 8491-8494, 2019/08/27 2019, doi: 10.1021/acsnano.9b06394.
[27] M. Naguib, V. N. Mochalin, M. W. Barsoum, and Y. Gogotsi, "25th Anniversary Article: MXenes: A New Family of Two-Dimensional Materials," *Advanced Materials*, vol. 26, no. 7, pp. 992-1005, 2014, doi: https://doi.org/10.1002/adma.201304138.
[28] K. Kannan, K. K. Sadasivuni, A. M. Abdullah, and B. Kumar, "Current Trends in MXene-Based Nanomaterials for Energy Storage and Conversion System: A Mini Review," *Catalysts*, vol. 10, no. 5, p. 495, 2020. [Online]. Available: https://www.mdpi.com/2073-4344/10/5/495.
[29] M. Han *et al.*, "Beyond Ti3C2Tx: MXenes for Electromagnetic Interference Shielding," *ACS Nano*, vol. 14, no. 4, pp. 5008-5016, 2020/04/28 2020, doi: 10.1021/acsnano.0c01312.
[30] L. Verger, V. Natu, M. Carey, and M. Barsoum, "MXenes: An Introduction of Their Synthesis, Select Properties, and Applications," (in English), *Trends in Chemistry*, vol. 1, no. 7, pp. 656-669, 2019-10 2019, doi: 10.1016/j.trechm.2019.04.006.
[31] N. Akhtar *et al.*, "Synthesis and characterization of MXene/ BiCr2O4 nanocomposite with excellent electrochemical properties," *Journal of Materials Research and Technology*, vol. 15, pp. 2007-2015, 2021/11/01/ 2021, doi: https://doi.org/10.1016/j.jmrt.2021.08.101.
[32] M. Nadeem *et al.*, "Structural stability, electronic structure, mechanical and optical properties of MAX phase ternary Mo2Ga2C, Mo2GaC and Mo3GaC2 carbides," *Journal*

of Materials Research and Technology, vol. 14, pp. 521-532, 2021/09/01/ 2021, doi: https://doi.org/10.1016/j.jmrt.2021.06.079.

[33] S. Sarikurt, D. Çakır, M. Keçeli, and C. Sevik, "The influence of surface functionalization on thermal transport and thermoelectric properties of MXene monolayers," *Nanoscale*, 10.1039/C7NR09144C vol. 10, no. 18, pp. 8859-8868, 2018, doi: 10.1039/C7NR09144C.

[34] A. Champagne and J.-C. Charlier, "Physical properties of 2D MXenes: from a theoretical perspective," *Journal of Physics: Materials*, vol. 3, no. 3, p. 032006, 2020/08/13 2021, doi: 10.1088/2515-7639/ab97ee.

[35] C.-L. Choong *et al.*, "Highly Stretchable Resistive Pressure Sensors Using a Conductive Elastomeric Composite on a Micropyramid Array," *Advanced Materials*, vol. 26, no. 21, pp. 3451-3458, 2014, doi: https://doi.org/10.1002/adma.201305182.

[36] M. Okubo, A. Sugahara, S. Kajiyama, and A. Yamada, "MXene as a Charge Storage Host," (in eng), *Acc Chem Res*, vol. 51, no. 3, pp. 591-599, Mar 20 2018, doi: 10.1021/acs.accounts.7b00481.

[37] M. Aakyiir *et al.*, "Stretchable, mechanically resilient, and high electromagnetic shielding polymer/MXene nanocomposites," *Journal of Applied Polymer Science*, vol. 138, no. 22, p. 50509, 2021, doi: https://doi.org/10.1002/app.50509.

[38] X. Jin *et al.*, "Flame-retardant poly(vinyl alcohol)/MXene multilayered films with outstanding electromagnetic interference shielding and thermal conductive performances," *Chemical Engineering Journal*, vol. 380, p. 122475, 2020/01/15/ 2020, doi: https://doi.org/10.1016/j.cej.2019.122475.

[39] A. Rozmysłowska-Wojciechowska *et al.*, "Engineering of 2D Ti3C2 MXene Surface Charge and its Influence on Biological Properties," *Materials*, vol. 13, no. 10, p. 2347, 2020. [Online]. Available: https://www.mdpi.com/1996-1944/13/10/2347.

[40] M. Aakyiir *et al.*, "3D printing interface-modified PDMS/MXene nanocomposites for stretchable conductors," *Journal of Materials Science & Technology*, vol. 117, pp. 174-182, 2022/08/01/ 2022, doi: https://doi.org/10.1016/j.jmst.2021.11.048.

[41] H. Yang *et al.*, "Wireless Ti3C2Tx MXene Strain Sensor with Ultrahigh Sensitivity and Designated Working Windows for Soft Exoskeletons," *ACS Nano*, vol. 14, no. 9, pp. 11860-11875, 2020/09/22 2020, doi: 10.1021/acsnano.0c04730.

[42] Y. Deng, Y. Shen, Y. Du, T. Goto, and J. Zhang, "A novel electrode hybrid of N–Ti3C2Tx/C/CuS fabricated using ZIF-67 as an intermediate derivation for superhigh electrochemical properties of supercapacitors," *Journal of Materials Research and Technology*, vol. 19, pp. 3507-3520, 2022/07/01/ 2022, doi: https://doi.org/10.1016/j.jmrt.2022.06.118.

[43] C. Ma, M.-G. Ma, C. Si, X.-X. Ji, and P. Wan, "Flexible MXene-Based Composites for Wearable Devices," *Advanced Functional Materials*, vol. 31, no. 22, p. 2009524, 2021, doi: https://doi.org/10.1002/adfm.202009524.

[44] Y. Lu *et al.*, "Highly Stretchable, Elastic, and Sensitive MXene-Based Hydrogel for Flexible Strain and Pressure Sensors," *Research*, vol. 2020, p. 2038560, 2020/07/14 2020, doi: 10.34133/2020/2038560.

[45] Q. Li *et al.*, "Flexible conductive MXene/cellulose nanocrystal coated nonwoven fabrics for tunable wearable strain/pressure sensors," *Journal of Materials Chemistry A*, 10.1039/D0TA07832H vol. 8, no. 40, pp. 21131-21141, 2020, doi: 10.1039/D0TA07832H.

[46] W. Yuan *et al.*, "MXene-composited highly stretchable, sensitive and durable hydrogel for flexible strain sensors," *Chinese Chemical Letters*, vol. 32, no. 6, pp. 2021-2026, 2021/06/01/ 2021, doi: https://doi.org/10.1016/j.cclet.2020.12.003.
[47] K. Yang, F. Yin, D. Xia, H. Peng, J. Yang, and W. Yuan, "A highly flexible and multifunctional strain sensor based on a network-structured MXene/polyurethane mat with ultra-high sensitivity and a broad sensing range," *Nanoscale*, 10.1039/C9NR00488B vol. 11, no. 20, pp. 9949-9957, 2019, doi: 10.1039/C9NR00488B.
[48] K. Zhang *et al.*, "Self-Healing Ti3C2 MXene/PDMS Supramolecular Elastomers Based on Small Biomolecules Modification for Wearable Sensors," *ACS Applied Materials & Interfaces*, vol. 12, no. 40, pp. 45306-45314, 2020/10/07 2020, doi: 10.1021/acsami.0c13653.
[49] Q. Guo *et al.*, "Protein-Inspired Self-Healable Ti3C2 MXenes/Rubber-Based Supramolecular Elastomer for Intelligent Sensing," *ACS Nano*, vol. 14, no. 3, pp. 2788-2797, 2020/03/24 2020, doi: 10.1021/acsnano.9b09802.
[50] S. Seyedin *et al.*, "MXene Composite and Coaxial Fibers with High Stretchability and Conductivity for Wearable Strain Sensing Textiles," *Advanced Functional Materials*, vol. 30, no. 12, p. 1910504, 2020, doi: https://doi.org/10.1002/adfm.201910504.
[51] Y. Xu *et al.*, "Flexible, fouling-resistant and self-cleaning Ti3C2Tx-derivated hydrophilic nanofiltration membrane for highly efficient rejection of organic molecules from wastewater," *Journal of Materials Research and Technology*, vol. 9, no. 5, pp. 11675-11686, 2020/09/01/ 2020, doi: https://doi.org/10.1016/j.jmrt.2020.08.031.
[52] S. Araby, Q. Meng, L. Zhang, I. Zaman, P. Majewski, and J. Ma, "Elastomeric composites based on carbon nanomaterials," *Nanotechnology*, vol. 26, no. 11, p. 112001, 2015/02/23 2015, doi: 10.1088/0957-4484/26/11/112001.
[53] S. Abazari *et al.*, "MgO-incorporated carbon nanotubes-reinforced Mg-based composites to improve mechanical, corrosion, and biological properties targeting biomedical applications," *Journal of Materials Research and Technology*, vol. 20, pp. 976-990, 2022/09/01/ 2022, doi: https://doi.org/10.1016/j.jmrt.2022.06.154.
[54] Y. Cai *et al.*, "Stretchable Ti3C2Tx MXene/Carbon Nanotube Composite Based Strain Sensor with Ultrahigh Sensitivity and Tunable Sensing Range," *ACS Nano*, vol. 12, no. 1, pp. 56-62, 2018/01/23 2018, doi: 10.1021/acsnano.7b06251.
[55] M. Alhabeb *et al.*, "Guidelines for Synthesis and Processing of Two-Dimensional Titanium Carbide (Ti3C2Tx MXene)," *Chemistry of Materials*, vol. 29, no. 18, pp. 7633-7644, 2017/09/26 2017, doi: 10.1021/acs.chemmater.7b02847.
[56] M. Aakyiir *et al.*, "Combining hydrophilic MXene nanosheets and hydrophobic carbon nanotubes for mechanically resilient and electrically conductive elastomer nanocomposites," *Composites Science and Technology*, vol. 214, p. 108997, 2021/09/29/ 2021, doi: https://doi.org/10.1016/j.compscitech.2021.108997.
[57] H. Li, R. Chen, M. Ali, H. Lee, and M. J. Ko, "In Situ Grown MWCNTs/MXenes Nanocomposites on Carbon Cloth for High-Performance Flexible Supercapacitors," *Advanced Functional Materials*, vol. 30, no. 47, p. 2002739, 2020, doi: https://doi.org/10.1002/adfm.202002739.
[58] C. Lin *et al.*, "MXene/air-laid paper composite sensors for both tensile and torsional deformations detection," *Composites Communications*, vol. 25, p. 100768, 2021/06/01/ 2021, doi: https://doi.org/10.1016/j.coco.2021.100768.

[59] L. Zhao, K. Wang, W. Wei, L. Wang, and W. Han, "High-performance flexible sensing devices based on polyaniline/MXene nanocomposites," *InfoMat*, vol. 1, no. 3, pp. 407-416, 2019, doi: https://doi.org/10.1002/inf2.12032.

[60] S. Xia, S. Song, F. Jia, and G. Gao, "A flexible, adhesive and self-healable hydrogel-based wearable strain sensor for human motion and physiological signal monitoring," *Journal of Materials Chemistry B*, vol. 7, no. 30, pp. 4638-4648, 2019.

[61] S. AlMahri, J. Schneider, A. Schiffer, and S. Kumar, "Piezoresistive sensing performance of multifunctional MWCNT/HDPE auxetic structures enabled by additive manufacturing," *Polymer Testing*, vol. 114, p. 107687, 2022/10/01/ 2022, doi: https://doi.org/10.1016/j.polymertesting.2022.107687.

[62] S. Kumar, T. K. Gupta, and K. M. Varadarajan, "Strong, stretchable and ultrasensitive MWCNT/TPU nanocomposites for piezoresistive strain sensing," *Composites Part B: Engineering*, vol. 177, p. 107285, 2019/11/15/ 2019, doi: https://doi.org/10.1016/j.compositesb.2019.107285.

[63] S. Yao and Y. Zhu, "Wearable multifunctional sensors using printed stretchable conductors made of silver nanowires," *Nanoscale*, vol. 6, no. 4, pp. 2345-2352, 2014.

[64] Y. Bu *et al.*, "Ultrasensitive strain sensor based on superhydrophobic microcracked conductive Ti3C2Tx MXene/paper for human-motion monitoring and E-skin," *Science Bulletin*, vol. 66, no. 18, pp. 1849-1857, 2021.

[65] L. Liu *et al.*, "High-Performance Wearable Strain Sensor Based on MXene@Cotton Fabric with Network Structure," *Nanomaterials*, vol. 11, no. 4, p. 889, 2021. [Online]. Available: https://www.mdpi.com/2079-4991/11/4/889.

[66] R. Liu *et al.*, "MXene-coated air-permeable pressure-sensing fabric for smart wear," *ACS Applied Materials & Interfaces*, vol. 12, no. 41, pp. 46446-46454, 2020.

[67] N. Li *et al.*, "High-Performance Humidity Sensor Based on Urchin-Like Composite of Ti3C2 MXene-Derived TiO2 Nanowires," *ACS Applied Materials & Interfaces*, vol. 11, no. 41, pp. 38116-38125, 2019/10/16 2019, doi: 10.1021/acsami.9b12168.